Synthesis of activated carbons from water hyacinth biomass and its application as adsorbents in water pollution control

AHMAD HAKKY MOHAMMAAD* and MIRJANA KIJEVČANIN#

University of Belgrade Faculty of Technology and Metallurgy, Karnegijeva 4, 11000 Belgrade, Serbia

Abstract: The water hyacinth biomass was used for the synthesis of activated carbons in a process of chemical activation with $ZnCl_2$, followed by controlled pyrolysis. The applied impregnation weight ratios $ZnCl_2$ and dry hyacinth biomass were in the range of 0.5–3.5. The carbonization was conducted at four different temperatures (400–700 °C) under an inert atmosphere. The highest yield of activated carbon was obtained for the impregnation ratio of 0.5 and carbonization temperature of 400 °C. The samples were characterized using elemental analysis, adsorption–desorption isotherms of nitrogen and SEM analysis. The activated carbon obtained with an impregnation ratio 2.0 and carbonization temperature of 500 °C ($2.0AC_{500}$) showed the highest values of specific surface area and total pore volume of 1317 m^2 g^{-1} and 0.697 cm^3 g^{-1}, respectively. The adsorption of glyphosate, pesticide with a strong negative environmental impact, was a fast process, with the equilibrium time of 120 min. The adsorption isotherms were fitted with Langmuir and Freundlich model. The Langmuir adsorption capacity of $q_{max} = 240.8$ mg g^{-1} for $2.0AC_{500}$ classified the selected adsorbent as a very efficient one. The tested adsorption process followed the kinetics of the pseudo-second-order model.

Keywords: carbonization; characterization; pyrolysis; pesticide removal; adsorption; modelling.

INTRODUCTION

One of the leading environmental problems in Africa and Asia is the presence of water hyacinth (*Eichhornia crassipes*) in natural waters (mostly rivers and lakes). Water hyacinth forms dense and impenetrable floating mats on water surfaces, causing considerable problems in aquatic ecosystems. This plant has shown a strong negative impact on the biodiversity of the aquatic system in many

ways: its presence leads to a significant reduction in the amount of light in the water, prevents access to wildlife (birds in particular) thereby disrupting the normal functioning of fauna and representing a suitable environment for mosquitoes breeding.[1]

Utilization of water hyacinth biomass as source of lignocellulose for the activated carbon production can be one of the strategies in water pollution control. Using activated carbon obtained from lignocellulose biomass instead of fossil coal will reduce the production of greenhouse gasses and therefore represents a green approach in the synthesis of materials that can be used in process of pollutant removal.[2] The water hyacinth is characterized by a high content of lignocellulose biomass, including 48 % hemicellulose as the major component, along with 20 % cellulose and with 10 % of average lignin content, so it can be potentially employed as a proper carbon source.[3–5]

The activated carbons have been used as adsorbents of a wide range of contaminants such as pharmaceuticals, metallic and non-metallic pollutants and dyes from aqueous solutions.[2,6] In comparison with other adsorbents (zeolites, clays and polymers) activated carbons show better performance and stability in terms of adsorption.[7] The chemical activation of raw lignocellulose precursor material is usually a one-step method for the activated carbons preparation. Among many chemical agents, the $ZnCl_2$ is one of the most effective chemicals used for producing activated carbons with highly developed porosity.[8,9] This activation agent has a high activating capability, and it is relatively expensive. In process of chemical activation, the $ZnCl_2$ contributes to the pore development by localized decomposition of organic matter, inhibiting tar formation and enhancing the carbon yield.[8,9]

Water hyacinth has already been used as a precursor for activated carbon synthesis. The activation processes were dominantly performed by KOH[10] or H_3PO_4[11] under various and well-studied experimental approach. On the other hand, $ZnCl_2$ activation of water hyacinth has been applied,[4,12] but the impact of amount of the activation agent has not been sufficiently studied.

Pesticides are chemical substances used for the increase of the agricultural production. As artificial organic compounds, pesticides can remain in the environment for many years and may be transported over a long distance.[13] Among many pesticides, glyphosate-based herbicides as systemic, broad-spectrum herbicides are widely used, therefore contributed to concerns about their environmental impact.[14] International Agency for Research on Cancer and World Health Organization classify glyphosate as substance that is "probably carcinogenic to humans" (group 2A).[15] According to the author's best knowledge, there is lack in the existing literature about application of activated carbons obtained from water hyacinth bio waste as adsorbents of glyphosate.

The main objective of the present work was to obtain activated carbons with a high surface area from water hyacinth biomass, using different amounts of $ZnCl_2$ and applying different carbonization temperatures. The selected activated carbon was further evaluated as adsorbent for glyphosate removal.

EXPERIMENTAL

Materials

The water hyacinth (WH) plant (Karbala, Iraq) was used as raw material for obtaining the activated carbon. The raw WH was washed with distilled water. The roots and stalks without leaves were chopped and dried in an oven for 24 h. The dried WH was boiled in 0.25 M hydrochloric acid to remove metallic oxides, rinsed with distilled water, and finally dried in vacuum freeze dryer for 24h. The dry WH was crushed and ground in rotary mill, and finally sieved in order to obtain particles sized 1.4–2.0 mm.

The $ZnCl_2$ (≥98 %), supplied from Sigma–Aldrich, was used as activating agent in process of chemical activation during the activated carbons synthesis.

The herbicide glyphosate – GPh (≥99 %), used in adsorption study, was purchased from Merck.

Activated carbons synthesis

The activated carbon (AC) based on dry water hyacinth biomass was prepared by chemical activation of dry WH with $ZnCl_2$ according to the procedure described in literature.[16] The impregnation ratio was calculated as the ratio of the weight of $ZnCl_2$ in solution to the weight of the dry WH. The impregnation ratio was 0.0, 0.5, 1.0, 1.5, 2.0, 2.5 and 3.0.

The 40 g of dry WH sample was added to 150 ml of solution with the appropriate mass of $ZnCl_2$ and stirred at 60 °C for 4 h. The solid and liquid phases were separated by filtration through Buchner funnel and dried at 105 °C during 24 h. The drying process was applied prior to carbonization in order to avoid the loss of sample caused by rash steam development. The carbonization of activated WC was carried out in electrical furnace with nitrogen flowing (150 cm^3 min^{-1}) and at heating rate of 15 °C min^{-1}. The carbonization during 80 min was conducted at following temperatures: 400, 500, 600 and 700 °C.

The obtained activated carbon was rinsed with 0.5 M HCl in order to remove the activating agent, washed with hot distilled water until neutral pH and finally dried at 110 °C for 12 h. The dry samples were weighted in order to calculate the yield.

The synthetized activated carbons were denoted according to impregnation ratio and carbonization temperature, e.g., $0.5AC_{400}$ means that the impregnation ratio and the carbonization temperature were 0.5 and 400 °C, respectively.

The yield of activated carbons was calculated from mass ratio between activated carbon and starting WH after drying process:

$$Y = 100 \frac{m_{AC}}{m_{dryWHAC}}$$ (1)

where Y / % is yield of the synthesis, m_{AC} / g is the mass of activated carbon and m_{dryWH} / g is the mass of dry WH.

Characterization methods

The synthetized ACs were characterized using elemental analysis, nitrogen adsorption-desorption isotherms and scanning electron microscopy (SEM).

The elemental analysis was used in order to determinate the content of carbon, hydrogen, nitrogen and sulphur in raw materials and activated carbons. The analysis was performed using elemental analyser instrument (Thermo Scientific – FlashEA1112 automatic elemental analyzers). Prior to analysis, the samples were dried in an oven at 110 °C.

The textural properties of activated carbons were obtained from adsorption-desorption nitrogen isotherms at –196 °C (Micromeritics' ASAP® 2020). Prior to analysis the samples were outgassed at 110 °C during 12 h. The specific surface area (S_{BET}) was calculated according to Brunner–Emmett–Teller method,[17] the total pore volume (V_T) was estimated from N_2 adsorption isotherm according to Gurvich rule, and represents the liquid molar volume adsorbed at pressure p/p_0 of 0.999.[18,19] The volumes of micropores and mesopores were calculated using Dubinin–Radushkevich method[20] and Barrett, Joyner, Halenda (BJH) method,[21] respectively.

The morphology of activated carbons was characterized by scanning electron microscopy (SEM-JEOL, JSM 6360 LV).

Adsorption study

The herbicide glyphosate (GPh) was used as a model of pesticide pollutant. During adsorption study, the GPh concentration was determined by UV–Vis spectrophotometer (UV–Vis 1800 Shimadzu) at $\lambda_{max} = 264$ nm.

The volume of GPh solution of 75 cm³ was introduced into the glass flasks and mixed with 20 mg of adsorbents. After the adsorption process, the GPh concentration in the supernatant was analyzed, with previous separation of the solid phase by centrifugation at 12,000 rpm for 20 min.

The effect of surface development of activated carbons on the adsorption efficiency was performed using GPh starting concentration of 100 mg dm⁻³ for the adsorption time of 240 min. The adsorption was performed from a solution with pH 3.55, which represents the unbuffered pH value of GPh solution for the investigated concentration.

The effect of contact time on the GPh adsorption was monitored at predetermined time intervals between 5 min and 240 min, at 25 °C, with starting GPh concentration of 100 mg dm⁻³.

The adsorption isotherms were constructed at equilibrium adsorption time at 25 °C with GPh initial concentration in range 50–250 mg dm⁻³.

The amount of the adsorbed herbicide (q_t / mg g⁻¹) was calculated according to:

$$q_t = \frac{(c_i - c_t)V}{m} \tag{2}$$

where c_i is the initial concentration of GPh /mg dm⁻³, c_t / mg dm⁻³ is the concentration of GPh in time t, V / dm⁻³ is the volume of GPh solution and m / g is the mass of the adsorbent.

Adsorption data analysis

Two well-known isotherm models Langmuir[22] and Freundlich[23] were used for modelling the adsorption data, while the adsorption kinetics data were fitted with both, pseudo-first[24] and pseudo-second order[25] kinetics' models. The applied isotherm and kinetics model have been frequently used for heterogeneous adsorption systems that consist of solid adsorbent and dissolved adsorbate molecule.[26]

RESULTS AND DISCUSSION

Results of characterization

The yield of activated carbons obtained after chemical activation with $ZnCl_2$ and carbonization process is given in Fig. 1.
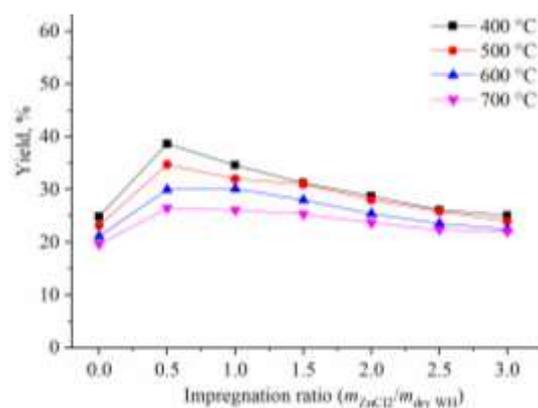

Fig. 1. The influence of impregnation ratio and carbonization temperature on yield of activated carbons prepared from water hyacinth dry material.

It was observed that activated carbons obtained with the impregnation ratio 0 (*i.e.*, without applied $ZnCl_2$) and the temperature range 400–700 °C had relatively low yield in the range of 19.6–24.9 %. This fact can be related to a high content of volatile matter and relatively low lignin content in raw WH material used for the preparation of activated carbons. According to the literature, the activated carbons obtained by pyrolisis without prior activation showed significant weight loss attributed to gasses extraction (CO, CO_2 and CH_4).[27] The activation agent and applied carbonization temperature have a significant impact on the yield of activated carbons (Fig. 1). Generally, the best yields were obtained for the lowest carbonization temperature (400 °C). With the temperature increase the yield of activated carbon decreased regardless the amount of applied $ZnCl_2$, which was explained by the promotion of tar volatilization by higher temperature.[28] For each carbonization temperature it was observed that the amount of the activation agent has a similar impact on yield, *i.e.*, the activated carbon yields continually decreased with the impregnation ratio higher than 0.5 (Fig. 1). This observation can be explained by larger evolution of volatiles compounds affected by dehydration agent – $ZnCl_2$.[29]

In order to estimate the effect of the amount of activation agent – $ZnCl_2$, on surface development, the specific surface area (S_{BET}) of samples obtained on the carbonization temperature of 400 °C was correlated with the impregnation ratio (from 0.0 to 3.0) and shown in Fig. 2.

The activated carbon obtained without impregnation showed the lowest value of S_{BET}. This result was expected since the $ZnCl_2$ works as a dehydration reagent during the carbonization process, which leads to carbon charring, form-

ations of the aromatic, porous structure, and restricts the formation of the tar.[29] The introduction of $ZnCl_2$ led to development of specific surface and this trend continued up to impregnation ratio 2.0, and after that decreased for higher impregnation ratios. These results are in accordance with literature data.[27,29,30]
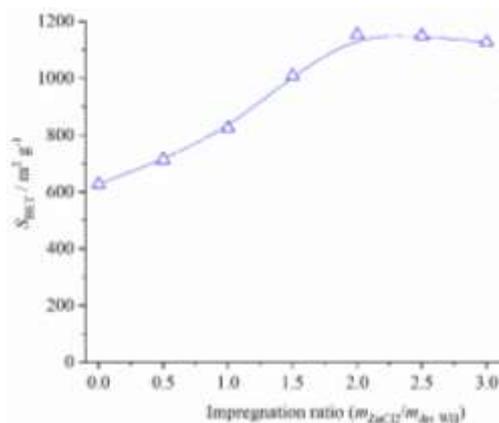

Fig. 2. The influence of impregnation ratio ($m_{ZnCl_2}/m_{dry\ WH}$) on specific surface area of carbons obtained by carbonization at 400 °C.

The more detailed textural properties analysis was applied on the activated carbon samples with impregnation ratio 2.0, since the carbons with highest S_{BET} values (Fig. 2) were obtained using $ZnCl_2$ in this impregnation ratio.

The effect of temperature (400–700 °C) on the specific surface area (S_{BET}), micropore (V_{mic}) and mesopore volume (V_{meso}) as well as on total pore volume (V_{tot}) of the activated carbons with impregnation ratio 2.0 are presented in Table I.

TABLE I. Surface area and pore volumes of activated carbons with impregnation ratio 2.0 obtained at different carbonization temperatures

T / °C	S_{BET} / m² g⁻¹	V_{tot} / cm³ g⁻¹	V_{mic} / cm³ g⁻¹	V_{meso} / cm³ g⁻¹
400	1154	0.602	0.301	0.298
500	1317	0.697	0.152	0.541
600	1284	0.670	0.135	0.527
700	1163	0.605	0.113	0.485

The most of the investigated textural properties increased with the rise of final carbonization temperature from 400 to 500 °C, while further increase of temperature led to surface development decreasing. Increasing temperature from 400 to 500 °C had strong positive impact on mesoporosity development, while temperatures higher than 500 °C led to slight decrease of mesopore volume. Besides that, all investigated carbonization temperatures above 400 °C reduced microporosity of activated carbons. Similar trends can be found in literature,[27,28,31] According to Rodriguez-Reinoso and Molina-Sabio,[27] $ZnCl_2$ has an important role in the development of micro- and mesoporosity in the carboniz-

ation process up to 500 °C, but at higher temperatures the reaction of $ZnCl_2$ with the char is negligible. The decrease in textural properties at temperatures higher than 500 °C can also be attributed to a sintering effect at high temperature, followed by the shrinkage of the char, and the realignment of the carbon structure.[32]

Sentilkumar *et al.*[12] applied the weight of $ZnCl_2$ that corresponded to 10 % of raw water hyacinth and the synthetized activated carbon with S_{BET} = 579.94 $m^2 g^{-1}$ at high temperature of 900 °C. Boonpoke[4] produced the microporous activated carbon with a specific surface area of 1066 $m^2 g^{-1}$ at 600 °C using an equal amount of $ZnCl_2$ and raw water hyacinth (impregnation ratio 1:1). The present study applied different amounts of $ZnCl_2$ and found that the impregnation ratio 2:1 leads to obtaining the activated carbons with higher values of S_{BET} than those in previous studies at lower carbonization temperatures of 400 and 500 °C (Table I). Wu *et al.*[10] activate the raw water hyacinth with KOH and synthetized activated carbon with S_{BET} = 1380 $m^2 g^{-1}$, but on 800 °C. Yang and Qiu[33] showed that the activated carbons with the specific surface area of even 2000 m^2 g^{-1} could be produced from pharmaceutics' herb residue, but synthesis required chemical activation with booth NaOH and $ZnCl_2$.

The elemental analysis was performed in order to evaluate the effect of temperature on the chemical composition of activated carbons. The result of the elemental analysis of dry WH and the activated carbons prepared with impregnation ratio of 2.0 are presented in Table II.

TABLE II. The results of the elemental analysis

Sample	Content of elements, wt. %				
	C	H	O^a	N	Ash
Dry WH	41.22	6.23	47.07	1.54	3.94
AC400	80.31	3.37	15.16	0.32	0.84
AC500	81.57	3.15	14.20	0.27	0.81
AC600	83.24	2.98	12.79	0.24	0.75
AC700	84.15	2.75	12.23	0.19	0.68

[a]The oxygen content is calculated from the difference up to 100 %

The major organic elements in all investigated samples are carbon and oxygen. The WH has higher content of ash, consisting mainly of silica and metal oxides.[16]

The treatment with HCl after activation process led to leaching of metal cations and therefore the ash content was reduced. During the carbonization process, with temperature rise the content of carbon increased, which was expected.[16]

The scanning electron microscopy (SEM) was employed to show the difference in the morphology between the raw WH material and the activated carbons with impregnation ratio 2:1, obtained in the temperature range from 400–700 °C.

The SEM images were recorded using magnification of 3000× and presented in Fig. 3.

In Fig. 3 significant difference in surface morphology can be observed between raw WH and ACs. The surface of the raw WH is moderately developed with parts of a smooth area, but after impregnation and carbonization, the raw WH biomass turns to be more porous with more open structures (Fig. 3). The increase of the carbonization temperature led to a reduction in small cracks in the activated carbon surfaces which could be responsible for the reduce of textural properties. According to the textural analysis the mesopore formation was dominantly responsible for the surface development (Table I). Since the mesopores are those with diameter from 2–50 nm, they are not visible in Fig. 3, where macroporous structure can be noticed.
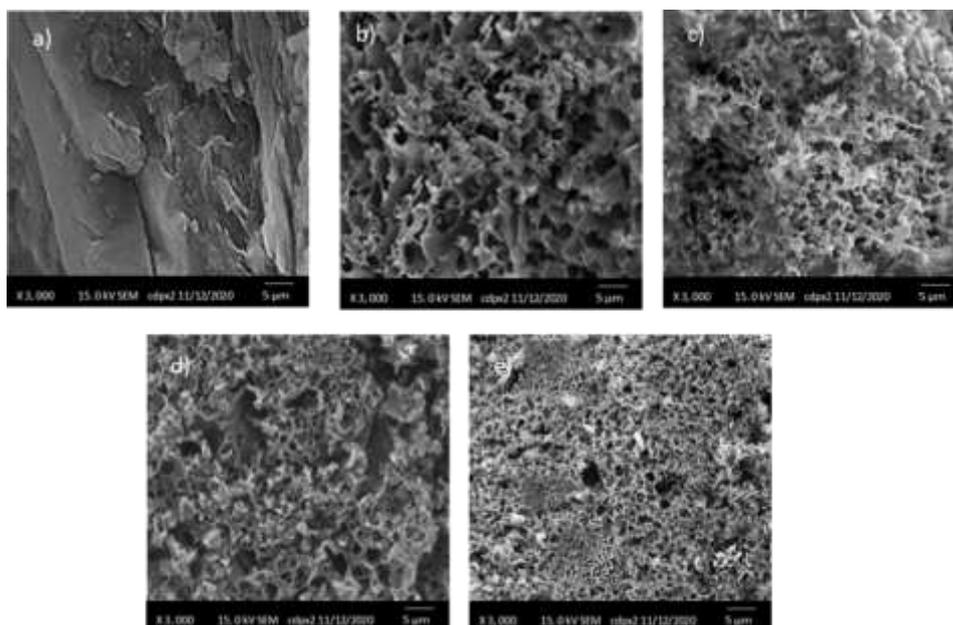

Fig. 3. The SEM images of: a) raw WH; b) $2.0AC_{400}$; c) $2.0AC_{500}$; d) $2.0AC_{600}$; e) $2.0AC_{700}$.

Adsorption study

The effect of surface development of activated carbons on adsorption efficiency. The aim of this adsorption study was to select the activated carbon with the best adsorption properties toward GPh. The effect of surface development of the activated carbons (impregnation ratio 2.0, T_{carb} = 400 to 700 °C) on the amount of adsorbed GPh for 240 min is presented in Fig. 4.

Although the specific surface area shows an impact on the amount of the adsorbed GPh, the difference in q_{240} for the samples with relatively close values

of S_{BET} was negligible. For example, the samples with S_{BET} values of 1317 and 1284 m^2g^{-1} adsorbed almost the same amount of GPh with values 153 and 151 mg g^{-1}, respectively. The obtained results suggested that the increasing S_{BET} values of ~30 m^2 g^{-1} did not lead to a significant increase in the efficiency of GPh removal. Herath et al[34] found that both physisorption and chemisorption mechanisms affected the adsorption of glyphosate onto the activated carbon, but that physical interactions dominantly increase with the rise of surface development.
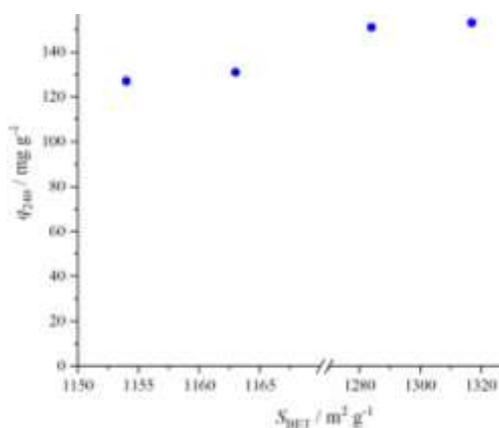

Fig. 4. The influence of specific surface area (S_{BET}) on the amount of the adsorbed glyphosate (q_{240}) for 240 min.

Although 2.0AC$_{500}$ and 2.0AC$_{600}$ showed almost the same amount of adsorbed GPh for the adsorption time of 240 min, the 2.0AC$_{500}$ was selected for further adsorption study, since its synthesis requires lower carbonization temperature.

Kinetic study

The effect of contact time on GPh adsorption on selected adsorbent 2.0AC$_{500}$ was performed in order to estimate the equilibrium time of adsorption (Fig. 5).

The uptake of GPh increased gradually up to 120 min and after this time the amount of adsorbed GPh was almost constant. For the investigated process, the time of 120 min can be considered as equilibrium, since there is no significant change in the amount of the adsorbed GPh for longer times. The amount of adsorbed GPh in equilibrium time was found to be q_e = 151.87 mg g^{-1}. In order to describe the kinetics of the process, the experimental data (Fig. 5) were fitted with pseudo-first and pseudo-second-order kinetic models. The calculated kinetic parameters for both models are given in Table III.

The results presented in Table III revealed that the experimental data show better fit with pseudo-second order kinetic model than with pseudo-first order model. The amount of adsorbed GPh in equilibrium calculated from pseudo-sec-

ond order kinetic model was q_e = 156.3 mg g^{-1} which is very close to the experimental value of q_e = 151.87 mg g^{-1}. According to many authors, pseudo-second order model indicates that the possible mechanism of investigated process included chemisorption of pollutants on adsorbent surface.[35]
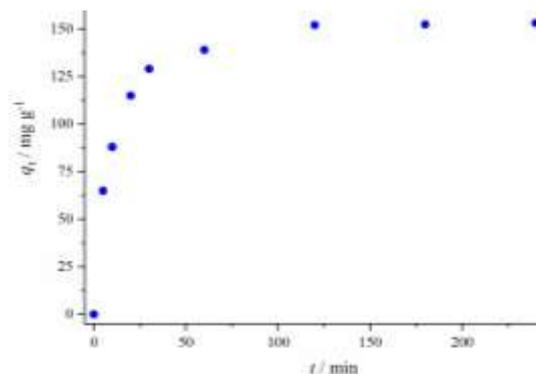

Fig. 5. The effect of contact time on GPh adsorption using activated carbon 2.0AC$_{500}$.

TABLE III. The parameters of pseudo-first and pseudo–second order kinetic models

Pseudo-first order	q_e / mg g^{-1}	k_1 / min^{-1}	R^2
	214.9	0.0773	0.944
Pseudo-second order	q_e / mg g^{-1}	k_2 / g mg^{-1} min	R^2
	156.3	0.0011	0.994

Adsorption isotherm models

The experimental isotherm data together with nonlinear fits of Langmuir and Freundlich models are presented in Fig. 6, while the calculated isotherm's parameters are listed in Table IV.
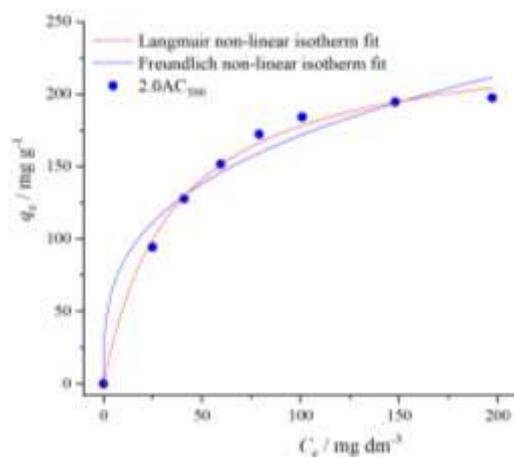

Fig. 6. The adsorption isotherm for GPh adsorption on 2.0AC$_{500}$ on 25 °C, fitted with Langmuir and Freundlich isotherm model.

Table IV. Calculated isotherm parameters for Langmuir and Freundlich model for GPh adsorption on $2.0AC_{500}$

Langmuir	K_L / dm^3 mg^{-1}	q_{max} / mg g^{-1}	R^2
	0.0284	240.8	0.995
Freundlich	K_F / (mg g^{-1})(dm^3 mg^{-1})$^{1/n}$	n	R^2
	41.15	3.23	0.965

Both investigated models generally could be applied to describe the GPh adsorption onto $2.0AC_{500}$ process, since coefficients of determination are $R^2 > 0.900$ (Table IV). However, the Langmuir model showed better fitting with the experimental data, having $R^2 = 0.995$. The agreement of adsorption data with Langmuir model indicated that surface of investigated adsorbent is energetically homogenous and the binding sites are uniformly distributed with the same affinity. The adsorption process occurs until monolayer surface coverage and after saturation there is no additional interaction between adsorbate molecules. The monolayer adsorption capacity (q_{max}) according to the Langmuir model was 240.8 mg g^{-1}.

The literature review of glyphosate adsorption on carbons derived from different type of biomass and other adsorbents is presented in Table V.

TABLE V. Comparison of glyphosate adsorption capacity of different adsorbents

Adsorbent	Adsorption parmeters	q_{max} / mg g^{-1}	References
$2.0AC_{500}$	$S_{BET} = 1317$ m^2 g^{-1};pH 3.55; $T = 25$ °C, C_{GPh}, 50–250 mg dm^{-3}	240.8	Current study
Rice husk char	$S_{BET} = 229$ m^2 g^{-1}; pH < 4; C_{GPh}, 0–100 mg dm^{-3}	123.03	34
Carbon derived from waste newspapers	$S_{BET} = 535$ m^2 g^{-1};pH 2.5; $T = 28$ °C; C_{GPh}, 5–100 mg dm^{-3}	48.4	36
Eucalyptus camaldulensis bark-mediatedchar	pH 10.18, $C_{GPh} = 20.28$ mg L^{-1}, contact time 78.42 min; $T = 303.23$ K	66.76	37
Carbon obtained from sugar cane bagasse	C_{GPh}, 0.338–2.704 g L^{-1}	161.3	38
Zr-MOF	pH 3–6; C_{GPh}, 20–70 mg L^{-1}; contact time: 1–180 min, T, 308–3018 K	256.54	39
Resin D301	T, 303.15–318.15 K; C_{GPh}, 5–50 mg/L; pH 4	833.33	40

Although Chen *et al.*[40] found that Resin D301 as adsorbent showed extraordinary efficiency for glyphosate removal, the adsorption capacity for $2.0AC_{500}$ of 240.8 mg g^{-1} is close to the adsorption capacity of Zr–MOF adsorbent[39] and still higher than q_{max} of the most reported carbon-based adsorbents. Therefore the $2.0AC_{500}$ could be classified as efficient and tested in real wastewaters treatments.

CONCLUSION

The water hyacinth biomass was used as starting material for the production of activated carbons. The activated carbons were synthetized using chemical activation with $ZnCl_2$ followed by controlled carbonization. On carbonization at various carbonization temperatures: 400, 500, 600 and 700 °C the different impregnation ratios of $ZnCl_2$ in range of 0.5–3.5 were applied. The chosen synthesis parameters showed significant impact on activated carbons yield and surface development. The impregnation ratio of 0.5 and temperature of 400 °C led to the highest yield of activated carbons. On the other hand, the textural properties showed that the most developed surface of 1317 m^2 g^{-1} and the total pore volume of 0.697 cm^3 g^{-1} has the activated carbon obtained with the impregnation ratio 2.0 and the carbonization temperature of 500 °C. This activated carbon with the best textural properties was used as an adsorbent for glyphosate, pesticide with strong negative environmental impact. Experiments showed that the adsorption takes place very fast and the equilibrium time was estimated at 120 min. The adsorption isotherms were fitted with Langmuir and Freundlich model, and Langmuir model showed better fit indicating that adsorption occurs in the form of monolayer on energetically equal and homogenously distributed adsorption sites. The Langmuir adsorption capacity of q_{max}=240.8 mg g^{-1} classified selected adsorbent as very efficient one. The adsorption kinetics study revealed that glyphosate adsorption follows the pseudo-second order kinetics, which indicates possible chemisorption mechanism.

ИЗВОД

СИНТЕЗА АКТИВНОГ УГЉА ИЗ БИОМАСЕ ВОДЕНОГ ЗУМБУЛА И ЊЕГОВА ПРИМЕНА КАО АДСОРБЕНАТА У КОНТРОЛИ ЗАГАЂЕЊА ВОДЕ

АХМАД ХАККУ МОХАММААD и МИРЈАНА КИЈЕВЧАНИН

Универзитет у Беоīраду Технолошко–метīалурīки факултīет, Карнеīијева 4, 11000 Беоīрад

Биомаса воденог зумбула је коришћена за синтезу активног угља у процесу хемијске активације са $ZnCl_2$, након чега је уследила контролисана пиролиза. Примењени масени односи импрегнације $ZnCl_2$ и суве биомасе зумбула били су у распону од 0,5–3,5. Карбонизација је спроведена на четири различите температуре (400–700 °C) у инертној атмосфери. Највећи принос активног угља добијен је за однос импрегнације 0,5 и температуру карбонизације 400 °C. Узорци су карактерисани применом елементалне анализе, адсорпционо–десорпционих изотерми азота и СЕМ анализе. Активни угаљ добијен за однос импрегнације 2,0 и температуру карбонизације 500 °C (2.0AC$_{500}$) показао је вредности специфичне површине и укупне запремине пора од 1317 и 0,697 cm^3 g^{-1}, редом. Адсорпција глифосата, пестицида са јаким негативним утицајем на животну средину, била је брз процес, са равнотежним временом од 120 min. Изотерме адсорпције су корелисане Langmuir и Freundlich моделом. Langmuir адсорпциони капацитет q_{max} = 240,8 mg g^{-1} за 2.0AC$_{500}$ класификовао је одабрани адсорбент као веома ефикасан. Тестирани процес адсорпције пратио је кинетику модела псеудо-другог реда.

(Примљено 21. децембра 2021, ревидирано 10. фебруара, прихваћено 11. фебруара 2022)

REFERENCES

1. M. A. Bote, V. R. Naik, K. B. Jagadeeshgouda, *Mater. Sci. Energy Technol.* **3** (2020) 397 (https://doi.org/10.1016/j.mset.2020.02.003)
2. M. Bilal, J. Ali, N. Hussain, M. Umar, S. Shujah, D. Ahmad, *J. Serb. Chem. Soc.* **85** (2020) 265 (https://doi.org/10.2298/JSC181108001B)
3. A. Saning, S. Herou, D. Dechtrirat, C. Ieosakulrat, P. Pakawatpanurut, S. Kaowphong, C. Thanachayanont, M. M. Titirici, L. Chuenchom, *RSC Adv.* **9** (2019) 24248 (https://doi.org/10.1039/C9RA03873F)
4. A. Boonpoke, *J. Environ. Biol.* **36** (2015) 1143 (http://www.jeb.co.in/journal_issues/2015 09_sep15/paper_15.pdf)
5. C. A. Riyanto, E. Prabalaras, *J. Phys.: Conf. Ser.* **1307** (2019) 012002 (https://doi.org/10.1088/1742-6596/1307/1/012002)
6. M. I. Din, S. Ashraf, A. Intisar, *Sci. Prog.* **100** (2017) 299 (https://doi.org/10.3184/003685017X14967570531606)
7. A. Regti, M. R. Laamari, S. E. Stiriba, M. El-Haddad, *J. Assoc. Arab Univ. Basic Appl. Sci.* **24** (2017) 10 (https://doi.org/10.1016/j.jaubas.2017.01.003)
8. Z. Hu, M. P. Srinivasan, *Micropor. Mesopor. Mater.* **43** (2001) 267 (https://doi.org/10.1016/S1387-1811(00)00355-3)
9. Z. Yue, J. Economy, *Micropor.Mesopor. Mater.* **96** (2006) 314 (https://doi.org/10.1016/j.micromeso.2006.07.025)
10. K. Wu, B. Gao, J. Su, X. Peng, X. Zhang, J. Fu, P. K. Chu, *RSC Adv.* **6** (2016) 29996 (https://doi.org/10.1039/C5RA25098F)
11. Y. Huang, L. Shunxing, C. Jianhua, Z. Xueliang, C. Yiping, A*ppl. Surf. Sci.* **293** (2014) 160 (https://doi.org/10.1016/j.apsusc.2013.12.123)
12. S. T. Senthilkumar, R. Kalai Selvan, Y. S. Lee, J. S. Melo, *J. Mater. Chem., A* **1** (2013) 1086 (https://doi.org/10.1039/c2ta00210h1086)
13. M. T. Scholtz, E. Voldner, A. C. McMillan, B. J. Van Heyst, *Atmos. Environ.* **36** (2002) 5005 (https://doi.org/10.1016/S1352-2310(02)00570-8)
14. M. Schweizer, K. Brilisauer, R. Triebskorn, K. Forchhammer, H. R. Köhler, *Peer J.* **7** (2019) 7094 (https://doi.org/10.7717/peerj.7094)
15. W. Morley, S. Seneff, *Surg. Neurol. Int.* **5** (2014) 134731 (https://doi.org/10.4103/2152-7806.134731)
16. T. H. Liou, *Chem. Eng. J.* **158** (2010) 129 (https://doi.org/10.1016/j.cej.2009.12.016)
17. J. Rouquerol, P. Llewellyn, F. Rouquerol, *Stud. Surf. Sci. Catal.* **160** (2007) 49 (https://doi.org/10.1016/S0167-2991(07)80008-5)
18. S. J. Gregg, K. S. W. Sing, *Adsorption, Surface Area, and Porosity 2*, Academic Press, London, 1982, pp. 41–105 (https://doi.org/10.1002/bbpc.19820861019)
19. F. Rouquerol, J. Rouquerol, K. Sing, *Absorption by powders and porous solids, Principles, Methodology and Applications*, Academic press, London, 1999, pp. 165–189 (https://doi.org/10.1016/B978-0-12-598920-6.X5000-3)
20. M. M. Dubinin, *J. Colloid Interface Sci.* **23** (1967) 487 (https://doi.org/10.1016/0021-9797(67)90195-6)
21. E. P. Barrett, L. G. Joyner, P. P. Halenda, *J. Am. Chem. Soc.* **73** (1951) 373 (https://doi.org/10.1021/ja01145a126)
22. I. Langmuir, *J. Am. Chem. Soc.* **40** (1918)1361 (https://doi.org/10.1021/ja02242a004)

23. H. M. F. Freundlich, *Z. Phys. Chem. A* **57** (1906) 385 (https://doi.org/10.1515/zpch-1907-5723)
24. S. Lagergren, *Handlingar* **24** (1898) 1 (https://doi.org/10.1002/andp.18983000208)
25. Y. S. Ho, J. C. Y. Ng, G. McKay, *Sep. Purif. Meth.* **29** (2000) 189 (https://doi.org/10.1081/SPM-100100009)
26. A. Ivanovska, L. Pavun, B. Dojčinović, M. Kostić, *J. Serb. Chem. Soc.* **86** (2021) 885 (https://doi.org/10.2298/JSC210209030I)
27. F. Rodriguez-Reinoso, M. Molina-Sabio, *Coloids Surfaces, A* **241** (2004) 15 (https://doi.org/10.1016/j.colsurfa.2004.04.007)
28. Q. Qian, M. Machida, H. Tatsumoto, *Bioresour. Technol.* **98** (2007) 353 (https://doi.org/10.1016/j.biortech.2005.12.023)
29. 29. S. Yorgun, N. Vural, H. Demiral, *Micropor. Mesopor. Mater.* **122** (2009) 189 (https://doi.org/10.1016/j.micromeso.2009.02.032)
30. A. C. Lua, T. Yang, *J. Colloid Interf. Sci.* **290** (2005)505 (https://doi.org/10.1016/j.jcis.2005.04.063)
31. M. M. Gómez-Tamayo, A. Macías-García, M. A. Díez, E. M. Cuerda-Correa, *J. Hazard. Mater.* **153** (2008) 28 (https://doi.org/10.1016/j.jhazmat.2007.08.012)
32. K. Mohanty, D. Das, M. N. Biswas, *Adsorption* **12** (2006) 119 (https://doi.org/10.1007/s10450-006-0374-2)
33. J. Yang, K. Qiu, *Chem. Eng. J.* **167** (2011) 148 (https://doi.org/10.1016/j.cej.2010.12.013)
34. I. Herath, P. Kumarathilaka, M. I. Al-Wabel, A. Abduljabbar, M. Ahmad, A. R. A. Usman, M. Vithanage, *Micropor. Mesopor. Mater.* **225** (2016) 280 (https://doi.org/10.1016/j.micromeso.2016.01.017)
35. B. H. Hameed, R. R. Krishni, S. A. Sata, *J. Hazard. Mater.* **162** (2009) 305 (https://doi.org/10.1016/j.jhazmat.2008.05.036)
36. M. M. Nourouzi, T. G. Chuah, T. S. Y. Choong, *Desalin. Water Treat.* **24** (2010) 321 (https://doi.org/10.5004/dwt.2010.1461)
37. K. Sen, J. K. Datta, N. K. Mondal, *Appl. Water Sci.* **9** (2019) 162 (https://doi.org/10.1007/s13201-019-1036-3)
38. D. C. Nguyena, A. I. Vezentseva, P. V. Sokolovskiyc, A. A. Greishc, *Russ. J. Phys. Chem., A* **95** (2021) 1212 (https://doi.org/10.1134/S0036024421060194)
39. Q. Yang, J. Wang, X. Chen, W. Yang, H. Pei, N. Hu, Y. Li, Y. Suo, T. Lic, J. Wang, *J. Mater. Chem.* **6** (2018) 2184 (https://doi.org/10.1039/C7TA08399H)
40. F. Chen, C. Zhou, G. Li, F. Peng, *Arab. J. Chem.* **9** (2016) S1665 (https://doi.org/10.1016/j.arabjc.2012.04.014).